Best Practices for Optimization of Phytoplankton Analysis in Natural Waters Using CytoSense Flow Cytometers

Clémentine Gallot, Zéline Hubert, Lumi Haraguchi, Hedy Aardema, Luis Felipe Artigas, Amel Bellaaj Zouari, Arnaud Cauvin, Raffaella Casotti, Véronique Créach, Georges Dubelaar, et al.

Cytometry Part A

ISAC CYTOMETRY Journal of Quantitative Cell Science PART A

ORIGINAL ARTICLE OPEN ACCESS

Best Practices for Optimization of Phytoplankton Analysis in Natural Waters Using CytoSense Flow Cytometers

Clémentine Gallot[1] | Zéline Hubert[2] | Lumi Haraguchi[3] | Hedy Aardema[4,5] | Luis Felipe Artigas[2] | Amel Bellaaj Zouari[6] | Arnaud Cauvin[2] | Raffaella Casotti[7] | Véronique Créach[8] | Georges Dubelaar[9] | Alexandre Epinoux[2] | Gérald Grégori[1] | Oliver Grosso[1] | Joanna Kolasinki[10] | Harrie Kools[9] | Rob Lievaart[9] | Arnaud P. Louchart[11] | Glaucia Moreira Fragoso[12] | Maialen Palazot[2] | Machteld Rijkeboer[13] | Kévin Robache[2] | Joseph Rolland[14] | Thomas Rutten[15] | Melilotus Thyssen[1]

[1]MIO, Institut Méditerranéen d'Océanologie, Aix Marseille Univ, Université de Toulon, CNRS, IRD, MIO, Marseille, France | [2]Laboratoire d'Océanologie et de Géosciences, UMR 8187 LOG, Université Littoral Côte D'Opale, CNRS, Université de Lille, IRD, Wimereux, France | [3]Research Infrastructure Unit, Finnish Environment Institute, Helsinki, Finland | [4]Department of Climate Geochemistry, Max Plank Institute for Chemistry, Mainz, Germany | [5]Department of Earth and Planetary Sciences, ETH Zürich, Zürich, Switzerland | [6]Laboratory of Marine Environment, National Institute of Marine Sciences and Technologies, Tunis, Tunisia | [7]Department of Marine Integrative Ecology, Stazione Zoologica Anton Dohrn, Napoli, Italy | [8]Centre for Environment, Fisheries and Aquaculture Science, Cefas, Lowestoft, Suffolk, UK | [9]CytoBuoy, Woerden, the Netherlands | [10]ENTROPIE, Écologie Marine Tropicale des Océans Pacifique et Indien, UMR 250 Université de La Réunion, IFREMER, CNRS, IRD, Université de Nouvelle Calédonie, Saint-Denis de La Réunion, France | [11]Department of Aquatic Ecology, Netherlands Institute of Ecology (NIOO-KNAW), Wageningen, the Netherlands | [12]Trondheim Biological Station, Department of Biology, NTNU, Trondheim, Norway | [13]Laboratory for Hydrobiological Analysis, Rijkswaterstaat (RWS), Lelystad, the Netherlands | [14]Université de Toulon, Aix Marseille Univ., CNRS, IRD, MIO, Toulon, France | [15]Thomas Rutten Projects, Middelburg, the Netherlands

Correspondence: Clémentine Gallot (clementine.gallot15@gmail.com) | Melilotus Thyssen (melilotus.thyssen@univ-amu.fr)

Received: 30 January 2025 | **Revised:** 18 September 2025 | **Accepted:** 23 September 2025

Funding: This study and preceding workshop come from EuroMarine TT-CYTO workshop, Excellence Initiative of Aix-Marseille University – A*MIDEX, European Commission's Horizon 2020 Research and Innovation program (Grant agreement No 101081642) and European Commission's H2020-INFRAIA (2019-1n871153 and 951799), French Prioritary Research Project RiOMar operated by the Agence Nationale de la Recherche (ANR) in the frame of France 2030 program (ProjetIA-22-POCE-0006), the French State and Hauts de France Regional frame contract project MARCO and IDEAL, supported by the graduate school IFSEA that benefits from a ANR IFSEA (ANR-21-EXES-0011) operated by the French National Research Agency, EU Marine Strategy Framework Directive (n2101893310), and European FEDER Fund (1166-39417).

Keywords: best practices | coincidence risk | CytoSense | detection optimization | flow cytometry | phytoplankton | quality control | regular maintenance

ABSTRACT

The use of flow cytometry to investigate phytoplankton functional groups is rapidly expanding worldwide, using lab- or ship-based instruments or autonomous environmental monitoring platforms. Automation, coupled with greater autonomy, allows for higher spatial and temporal resolution of phytoplankton groups, enhancing understanding of their dynamics and patterns, generating large datasets. The level of resolution is determined by both instrumental capabilities and optimization of its acquisition settings. Sharing these datasets with the scientific community, whether to improve global phytoplankton distribution resolution or facilitate the intercomparison of environmental indicators among monitoring laboratories, strongly relies on quality-controlled instruments and standardized data acquisition and analysis. This article focuses on CytoSense-type (CytoBuoy, NL) flow cytometers, which operate by recording the optical pulse shapes of particles as they pass through a laser beam. Different configurations such as laser wavelength and power, sheath fluid management, sample inlet design, and dataset output format were not considered, in order to focus on optimization and protocol standardization to resolve the whole phytoplankton size spectrum, from the smallest autofluorescing prokaryotes to colonies and chain-forming species. In this study, coincidence, PMT

voltage, trigger threshold optimization, and regular quality control procedures are considered and discussed, using datasets from three types of instruments and two contrasted marine coastal waters as case studies. The primary goal of this study is to establish a framework to guide and support the exploration and application of this type of flow cytometer, ultimately achieving a reliable and optimal resolution for sample acquisition of natural waters.

1 | Introduction

Historically, flow cytometers have been developed for biomedical applications [1]. Planktonic microorganisms, as particles suspended in a fluid, are well-suited for single-cell analysis by high-throughput flow cytometry and for this reason the earliest and most well-known application of flow cytometry within aquatic sciences has been the investigation of phytoplankton ([2, 3]). Since then, flow cytometry has spread worldwide and has led to remarkable new insights into aquatic ecosystems such as the discovery of the importance of the picophytoplankton (<2–$3\,\mu m$). This technique is ideal to address phytoplankton patchiness [4–8], functional diversity [9, 10], and cell cycle dynamics [11, 12]. Benchtop flow cytometers have been installed aboard scientific vessels, but their effectiveness has often depended on the availability of operators to collect and acquire discrete measurements. In response to the scientific community's need to better resolve the spatial and temporal distribution of marine microorganisms, advancements in technology, electronics, and informatics have led to the development of more compact and robust instruments, enabling autonomous field deployments. Most of them are suited to remote operations and are routinely used during sampling cruises either in a semi-continuous way by analyzing pumped sea water, or submerged, sampling the surrounding water. Several instruments have been commercialized, one can cite the CytoSense [13], the FlowCytoBot [12, 14], and the SeaFlow [15, 16]. As a consequence, flow cytometry data have become a core parameter in most oceanographic investigations and are increasingly used for time-series on moorings and buoys. CytoSense-type instruments (including the CytoSub, CytoBuoy NL) have been used in marine research for over 20 years. Their advantage lies in the ability to resolve a wide size range, enabled by a large analyzed sample volume and a broad inlet, and to record complete optical pulse shapes for each particle, all integrated with an in-flow imaging system. Applications of such flow cytometers are numerous: spatio-temporal monitoring of natural communities for time series [17–20], surface submesoscale distribution [21–24], detection of Harmful Algae Bloom (HAB; [25]) and dynamics [26], trait analysis [9, 27], effects of particle transport and dust deposition [28, 29] as well as pollutants [30].

The successful discrimination of aquatic planktonic microorganisms by flow cytometry stems from a solid understanding of phytoplankton physiology, flow cytometry principles and the ability to maximize the instruments' resolution capabilities. The smallest photosynthetic group is commonly assigned taxonomically to *Prochlorococcus* [31]. In contrast, heterotrophic prokaryotes, which are of a similar size, require prior staining with a fluorescent dye targeting a cellular component, most often nucleic acids. Proper calibration and parameter tuning can ensure the sensitivity needed to accurately quantify such small organisms and their dynamics in an aquatic ecosystem.

As such, protocol standardization and best practices are essential to ensure proper instrument set up and operation, required to optimize its use in any natural aquatic environment. To date, flow cytometry best practices have primarily been developed for staining cells or particles under controlled laboratory conditions for medical research, focusing on optimizing setups and controls [32], or more specifically, for use in plant studies [33]. Recommendations for applying flow cytometry to natural water microorganisms have been suggested [34–37], leading to the establishment of a common vocabulary to describe the main groups observed in marine waters [38] and improved strategies for data management [39].

However, comprehensive recommendations and straightforward best practices to optimize settings and apply strategic quality controls to ensure reliable datasets have yet to be established for specific instruments such as in our case, CytoSense-type instruments, an operational pulse shape-recording flow cytometer. This study aims to provide guidelines for optimal data collection of natural phytoplankton communities both for the user's own objectives and for enhanced intercomparability. Instead of providing exact settings, it shares concepts, offers recommendations and guidance and raises potential issues during analysis.

2 | Experimental Context

2.1 | Samples Origin and General Technical Considerations

This study incorporated experiments designed to establish procedures using two types of CytoSense flow cytometers, analyzing separately samples from two contrasted areas, the Mediterranean Sea and the Eastern English Channel. A third instrument was also included in this study to illustrate a section on regular bead analysis for instrument monitoring. Instrument specifications are provided in Table 1.

CytoSense instruments were operated using the dedicated CytoUSB software, while data analysis was performed with CytoClus 5. All instruments included an image-in-flow device.

To perform instrument tests on CytoSense instrument CS-2015-68, samples were collected at the SSL@MM (Sea Water Sensing Laboratory @ MIO Marseille, Mediterranean Institute of Oceanology; 43.2805° N, 5.3492° W) station and at the SOMLIT point (43.2417° N, 5.29167° E) in the Bay of Marseille (France) coastal zone. This area is defined as oligotrophic, with relatively low nutrient concentrations [40] and low phytoplankton abundance, dominated by small-sized and low fluorescing cells, mostly picoplankton [41, 42].

To perform instrument tests on CytoSense instrument CS-2019-93, samples were collected along a nearshore-offshore

TABLE 1 | Specifications of the instruments used for the study.

Instrument reference and location	Year of construction	Laser (wavelength and power)	Channels (wavelength)
CS-2015-68 Marseille, France	2015	488 nm–120 mW	• FWS (left and right) • SWS (488 nm) • FLO (552–652 nm) • FLR (> 652 nm)
CS-2019-93 Wimereux, France	2019	488 nm–60 mW	• FWS (left and right) • SWS (488 nm) • FLY (536–601 nm) • FLO (604–664 nm) • FLR (688–726 nm)
CS-2019-97 Helsinki, Finland and Travemünde, Germany	2019	Laser 1: 488 nm–120 mW Laser 2: 596 nm–60 mW	• FWS (left and right) • SWS (488 nm) • FLG (502–538 nm) • FLY (553–577 nm) • FLO (604–644 nm) • FLR (668–726 nm)

transect (DYPHYRAD, [18, 43]) by the strait of Pas de Calais, close to the LOG (Laboratoire d'Océanologie et de Géoscience, Wimereux, France). The Eastern English Channel coastal area is meso- to eutrophic, with variable salinity values as related to river flows (Seine, Somme, Authie, Canche, Liane, Wimereux, Slack) forming a coastal stream, drifting northeast [44]. Phytoplankton is dominated by pico- and nano-sized cells [18, 21, 27] with a recurrent spring bloom of *Phaeocystis globosa* [45–47]. No *Prochlorococcus* are found in this area [48]. A third flow cytometer was used, CS-2019-97 (operated by the Finnish Environment Institute, Syke), which was deployed on a commercial ferry (M/S Finnmaid) between Helsinki, Finland and Travemünde, Germany. This instrument ran regular two-sized bead analysis and was used as practical examples of data acquisition.

2.2 | Common Vocabulary and Group Definition

In this study, phytoplankton cells analyzed by flow cytometry were grouped based on their optical similarities according to the vocabulary proposed by Thyssen et al. [38]. "Non-phytoplankton events" were defined based on the Total FWS bead signal of 1 μm silica beads, rendering two differentiated classes:

- "events larger than 1 μm beads" (mostly large detrital particles or small predators like ciliates, or decaying phytoplankton cells that have lost their pigments),
- "events smaller than 1 μm beads" (e.g., non-fluorescing heterotrophic prokaryotes, particulate matter, noise, or decaying cells).

Both events set a baseline from which the auto-fluorescing particles have to be separated.

The "events larger than 1 μm beads" density partly depends on the studied environment and the abundance of non-auto-fluorescing suspended particles. "Events smaller than 1 μm beads" were identified by analyzing the sheath fluid alone as a blank. Their occurrence increased when analyzing a natural sample, due to additional optical scattering from the core and non-auto-fluorescing particles. *Prochlorococcus* cells were of particular interest in this study, and adjusting instrument acquisition parameters (PMT voltage and trigger threshold) could improve resolution and separation over "non-phytoplankton events" signature. Most of these different groups are illustrated in Figure S1.

3 | Best Practices

3.1 | Maintenance Protocols and Quality Control

Prior to experimentation, maintenance and quality control procedures were conducted on the instruments. Technical procedures, such as laser and core alignment, tubing replacement, and filter replacement, were carried out according to the manufacturer's instructions and are not detailed in this manuscript. Similarly, this study does not address sampling methods, long-term deployments strategies or data analysis. Only fresh, unstained, and unstored natural samples were used to develop these Best Practices.

3.1.1 | Bead Protocols and Recommendations for Signal Stability Verification

Fluorescent polystyrene or non-fluorescing silica beads of various sizes should be routinely used. Ideally, they are included in each sample or before and after each measurement series to assess the stability of the laser power output and instrument's fluorescence and scattering detection over time.

An illustration of a stability check on instrument CS-2019-97 is presented in Figure 1. Beads were analyzed at regular time intervals, as the instrument was set up on a ferry, between March and October 2024. For this specific case, beads of two different sizes

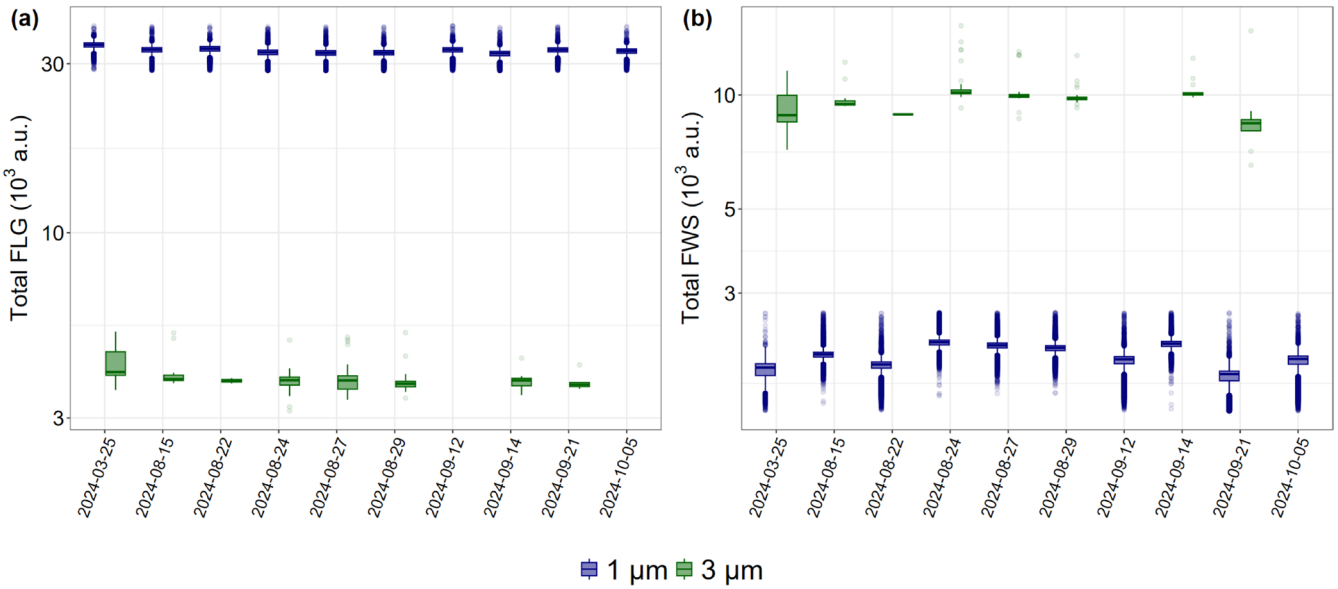

FIGURE 1 | Boxplots of the 1 µm (blue) and 3 µm (green) polystyrene bead distributions, regularly analyzed with instrument CS-2019-97 from March to October 2024 during a ferry deployment between Helsinki (Finland) and Travemünde (Germany): (a) Total Green Fluorescence (a.u.) and (b) Total Forward Scatter (a.u.) distribution. Each boxplot corresponds to one acquisition. [Color figure can be viewed at wileyonlinelibrary.com]

were used in the automated bead dispenser (a filled syringe with a magnetic homogenization system) of the instrument: 1 µm Thermofisher FluoSpheres Carboxylate-Modified Microspheres and 3 µm Biolegend Rainbow Fluorescent Particles, 1 peak (3.0–3.4 µm) – Bright Intensity. The solutions were prepared as follows: a suspension solution of MilliQ water with 0.01% NP-40 surfactant (Thermo Scientific NP-40 Detergent Surfact-Amps Solution) and 250 ppm of Proclin950 (Proclin Sigma-Aldrich). The bead stock solutions were resuspended and 5 drops of the 1 µm beads and 10 drops of the 3 µm beads were added into 10 mL of suspension solution. For other commercial solutions available, this proportion must be adjusted according to the respective starting concentration.

In this example, the green fluorescence threshold used for triggering the acquisition was set to 80 mV (FLG 80), and the acquisition time was 1.5 min at a sample speed of 1.08 µL s^{-1}.

Figure 1 displays a relatively stable distribution of the Total FLG (a.u.) and Total FWS (a.u.) for the two sizes of beads. The ratios between the medians of the two sizes showed stability in between the beads. In this example, two dates are missing for the 3 µm beads, as users ran out of stock solution during automated bead dispenser refilling.

Changes in beads optical values may result from factors such as laser mis-alignment or reduced power (e.g., lower excitation), mechanical shock, air bubbles stacked in the injector, gradual displacement of any part of the injector or the optics, or issues with the bead solution itself. They may also indicate a shift in sheath fluid flow rates, which could alter bead velocity and, consequently, the excitation time in the laser beam and the duration of data collection.

Significant changes observed in the optical values of the beads highlight the need to check optics (laser alignment, laser power) and the position of the flow core (following manufacturer instructions). Normalizing phytoplankton optical values to those of the beads corrects for minor optical shifts caused by the hardware.

Therefore, including beads in every analyzed sample is strongly recommended and can now be accomplished using the automated bead injection feature available in the most recent instruments. Running out of the stock solution during long term or remote deployments may occur, and the recommendation can be reduced by adjusting bead injection to one measurement per day depending on deployment length. As beads are stored in a syringe inside the instrument, a concentrated solution should be used in 0.2 µm filtered fresh water supplemented with biocide (such as Proclin Sigma-Aldrich, 0.03% to 0.1% recommended by the manufacturer) as well as a surfactant (in our example NP-40), to minimize bead aggregation and adhesion to the syringe walls.

Finally, beads stored in an automated dispenser or a plastic tube are not suitable for counting validation due to sedimentation, aggregation, and electrostatic interactions between the beads and the container. A suited protocol addressing counting validation considerations, such as electrostatic charge of the bead solution has been suggested by Marie et al. [49].

3.1.2 | Sample Pump Calibration

Calibrating the sample pump is essential for controlling the precise sample volume taken by the flow cytometer during analysis and obtaining reliable cell abundance measurements. Weighing a liquid with known density or obtaining the exact volume of a water aliquot can be performed manually by determining the mass of a 1 mL subsample. The exact volume analyzed can then be calculated. This is done by weighing the sample before and after a defined pumping period and comparing the result with the theoretical volume expected (pump speed measurement

time). If no precision scale is available at the sampling site/vessel, measuring a pumped volume can also be done using a precise syringe filled with a known volume. These checks should be performed regularly (e.g., before an experiment or survey). If the result is inaccurate compared to the expected pumped volume, calibration via CytoUSB is recommended.

3.1.3 | Instrument Cleaning and Biofouling Limitation

The sheath fluid should have a salinity similar to that of the analyzed sample to prevent shifts in refractive index, which can alter the trajectory of photons scattered or emitted by the particles as they pass through the sheath and sample core to reach the photodetectors. In the case of a recycled sheath fluid such as found in the CytoSense, a biocide such as Proclin (Sigma-Aldrich, 0.03% to 0.1% recommended by the manufacturer) should be added to prevent any biological development in the tubing, fluidics and flow cell. When possible, regular sheath fluid changes are recommended, even during high-frequency continuous measurements. Before storing an instrument for more than a week without usage, if the sheath fluid is composed of filtered seawater, it must be changed to ultrapure or deionized water as evaporation generates salt crystals clogging the tubing.

Complying with the manufacturer's instructions, the sheath tubing can be checked for contamination and eventually replaced. The same holds true for the filters installed in a sheath self-cleaning loop, when a slow but constant increase in pressure (monitored and displayed continuously on the software) is observed during acquisition. In case of high and unexpected scattering signals, the quartz flow cell may require cleaning following the manufacturer's recommendation.

3.2 | Acquisition Settings Optimization: Counting and Resolving the Full Phytoplankton Size Range

3.2.1 | Maximal Counting Rate – Coincidence Risk

Coincidence occurs when two or more events cross the laser beam at the same time or too closely to be discriminated separately and are therefore counted as a single event [35]. Increasing the event rate also increases the probability of coincidence. At high rates, events may occur too close together to be distinguished, either due to overlap or the limited processing speed of the electronics defined as the *dead time* of the instrument [1]. For accurate particle count, cells must be properly separated from each other to be intercepted by the laser individually, by keeping a sufficient distance between them. Coincidence risks are increased when a sample is highly concentrated (e.g., bloom event, cultures, turbid water) and with large particle length (e.g., many filamentous particles), or increasing flow rate.

Coincidence phenomenon was tested on CS-2015-68 by running dilution experiments with bead solutions. Samples were analyzed in 3 mL and dilution factors of the initial concentration ranged from 100% to 5%. The stock solution consisted of two drops of industrial bead solution (2.0 μm Fluoresbrite Polychromatic Red Microspheres, PolySciences) diluted in 40 mL of filtered seawater (0.2 μm). *Please note that such experiment will temporarily leave beads in the instrument's tubing.*

Bead concentrations were then extracted from the data files using CytoClus 5 software as a function of the various dilution factors. Theoretical concentrations, correcting for the experimental dilution factor, were calculated from the lowest measured abundance as the bead's initial concentration was unknown. The difference was calculated as a percentage (%) between the actual and expected counts.

Bead solutions of different concentrations were run for three minutes at three different sample flow rates of 3, 5, and 10 $\mu L\,s^{-1}$. Illustrating the measured event rate as a function of the theoretical event rate highlights the difference between them (Figure 2a,b,c). For instrument CS-2015-68, a 10% difference occurs at ~3,300 events s^{-1} for the 3 $\mu L\,s^{-1}$ flow rate and at ~3,100 events s^{-1} for the 5 $\mu L\,s^{-1}$. The event rate at 10 $\mu L\,s^{-1}$ is inconclusive, as the 10% difference appears from the very first data point, indicating insufficient precision. Newer instruments (series CS > 85) have improved hardware and software, and dead time may have shortened. For instance, CS-2019-93 did not evidence any difference between expected and counted beads at 5000 events s^{-1} at a flow rate of 5 $\mu L\,s^{-1}$ (data not shown).

Using the CytoUSB software, it is possible to include in the sampling protocol an automatic flow rate adjustment. This feature offers a practical solution for remote sampling scenarios, where manual sample dilution or trigger level adjustments are not feasible. If an acquisition starts to be affected by a high level of coincidence, even after automatic adjustment of the sample pump, and results in a sample volume of only a few hundred microliters or less for picoplankton, the sample may be flagged as being of poor quality. No consensus exists in the literature regarding a minimum acceptable acquisition volume, as counting will be limited by its value rather than the acquired volume.

However, in natural waters, the cell abundance required to reach coincidence, as demonstrated for CS-2015-68 in Figure 2, is of approximately 10^6 cells mL^{-1} (based on 3300 events s^{-1} over 300 s at a flow rate of 3 $\mu L\,s^{-1}$). Such abundances are rarely encountered in natural environments, suggesting that adjusting the sample pump speed is generally unnecessary. If coincidence is observed, it is more likely due to high levels of chromophoric dissolved organic matter, contamination increasing "non-phytoplankton events", or excessive scattering due to optical misalignment.

3.2.2 | Detection Settings: Examples From Natural Seawater Experiments

Optimizing phytoplankton detection via flow cytometry involves both detecting the signal and separating it from "non-phytoplankton events", especially from "events smaller than 1 μm beads" [50]. Signal detection depends on the trigger threshold, which defines when the instrument begins recording an event. Detection sensitivity, or the ability to separate dim fluorescing cells from "non-phytoplankton events", is in part influenced by the type of PMT and the voltage applied to them. To simplify operations, as PMTs can be individually adjusted,

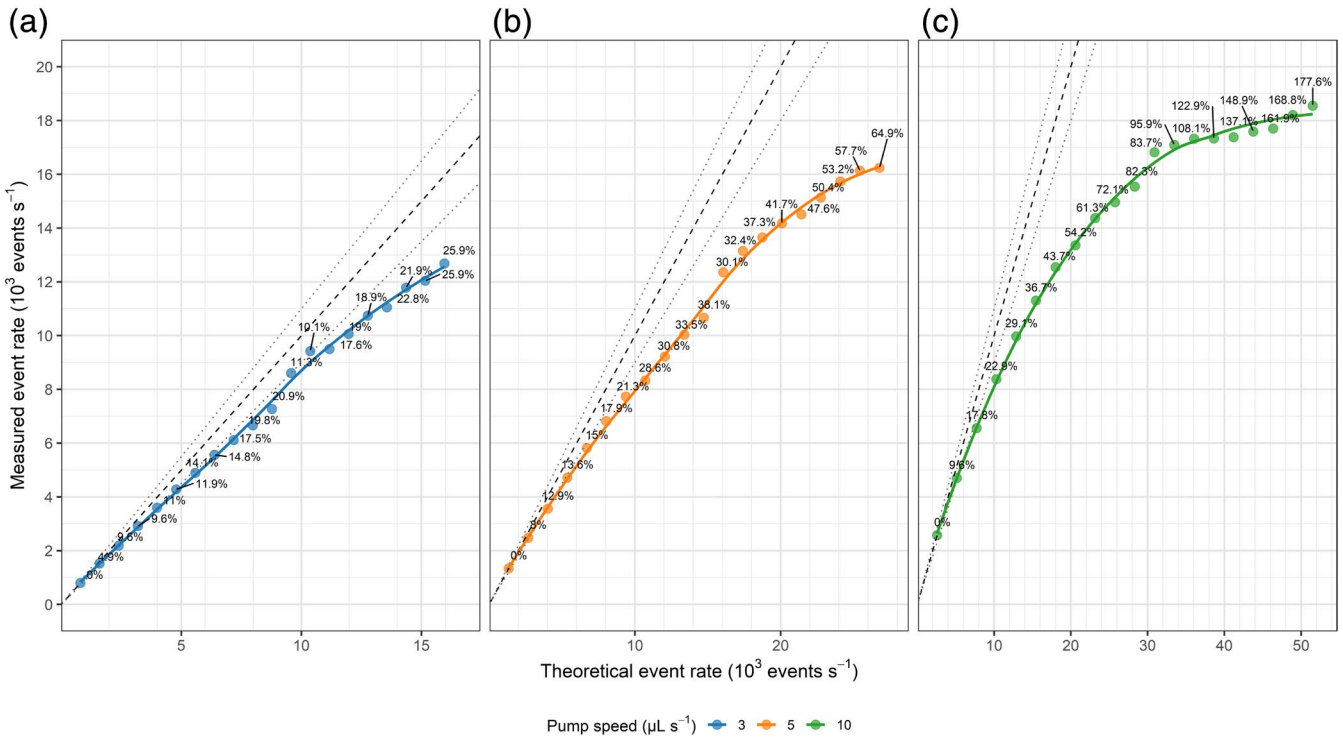

FIGURE 2 | Measured versus theoretical event rates of 2 µm red fluorescence beads (10^3 events s^{-1}) during a dilution experiment at three different sample flow rates: (a) 3 µL s^{-1}, (b) 5 µL s^{-1}, and (c) 10 µL s^{-1} (CS-2015-68). The gray dotted line is the 1:1 expected relationship surrounded by the 10% difference. The numbers next to each data point correspond to the percent difference of the theoretical event rate from the measured event rate per dilution (%). [Color figure can be viewed at wileyonlinelibrary.com]

CytoBuoy provides three PMT presets in CytoUSB: "Low", "Medium", and "High".

This section aims to establish the ideal measurement settings, combining trigger threshold and PMT voltage, ensuring accurate detection of all potentially targeted phytoplankton communities, particularly the smallest and/or dimmest in fluorescence. It is indeed essential to consider the size range of the targeted cells and the challenge associated with accommodating both ends of the spectrum when describing a phytoplankton community. Groups of small, dimly fluorescent cells, such as *Synechococcus* or *Prochlorococcus* (hereafter, OraPicoProk and RedPicoProk), may be missed or only partially recorded if the trigger threshold of the dedicated detector or the PMT voltage are not appropriately set. Despite optimizing PMT voltage and trigger levels, it can still be difficult to accurately count RedPicoProk. As such, Jiao et al. [51] evidenced a variation in red fluorescence on a 10-fold range for RedPicoProk cells, making them undetectable, or causing overlap with "non-phytoplankton events", particularly in surface waters exposed to daylight. Finally, optimization of the instrument does not necessarily mean analyzing the whole size spectrum, but rather that the instrument has reached its maximal performance capacities.

3.2.2.1 | Trigger Threshold Optimization. Whether protocols are triggering on red fluorescence (FLR, a.u.), sideward scatter (SWS, a.u.), a combination of both (smart triggering), or any other emitted light, a compromise must be found between lowering trigger levels and maintaining signal above the instrument's "non-phytoplankton events" signature threshold (all while avoiding coincidence).

When targeting natural phytoplankton communities from unstained samples, it is recommended to begin optimizing the trigger threshold on fluorescence channels, starting with red fluorescence induced by chlorophyll *a*, followed by SWS, related to size and structure (granularity) of the particles. However, using SWS can generate files filled with non-targeted particles, hiding the sought signal of phytoplankton, or generating data-heavy files (longer processing time). Initial trigger threshold optimization was performed with PMTs set to "Medium".

3.2.2.1.1 | Step 1: Sheath Fluid Signal – Blank Reference. Identifying the sheath fluid signal in both fluorescence and scatter is essential for estimating the boundary of "non-phytoplankton events", as the sheath fluid signature serves as reference. It will mainly concern "events smaller than 1 µm beads" as the sheath is recycled through 0.1 down to 0.05 µm filters. To determine the lowest limits of the instrument's trigger threshold, an acquisition is conducted running only the sheath fluid used during the analysis. When the sheath fluid, the sample pump tubing, and the overall fluidics and cuvette are clean, it is easier to determine the lowest trigger level as it reduces "non-phytoplankton events". To run a blank measurement and find the blank reference settings, the sample pump is manually stopped by changing the speed to 0.0 µL s^{-1}. As such, there is no sample core in the flow cell. Trigger thresholds can be modified in real-time by enabling a change of settings during acquisition ("Enable" function in Instrument Control tab in CytoUSB) to highlight "non-phytoplankton events". This range of tested trigger thresholds on the sheath fluid is required to have a preliminary idea on the set of thresholds to test on natural samples.

TABLE 2 | Analyzed volume (mL) and abundance (cells mL^{-1}) of the smallest phytoplankton group and event rate (events s^{-1}) illustrated on Figure 3, depending on different trigger level for the two instruments (CS-2015-68 and CS-2019-93).

Instrument	Trigger level (mV)	Analyzed volume (mL)	PFG	Abundance (cells mL^{-1}) mean ± SD $n = 3$	Event rate (events s^{-1})
CS-2015-68	FLR 5	0.014	OraPicoProk RedPicoProk	Not estimated Not estimated	28609 ± 2704
CS-2015-68	FLR 6	0.405	OraPicoProk RedPicoProk	4020 ± 277 7630 ± 651	136 ± 16
CS-2015-68	FLR 7	0.448	OraPicoProk RedPicoProk	4011 ± 192 5485 ± 536	42 ± 4
CS-2015-68	FLR 8	0.447	OraPicoProk RedPicoProk	3348 ± 74.7 3137 ± 97.4	30 ± 0.58
CS-2019-93	FLR 1	0.531	OraPicoProk	9633 ± 136	3781 ± 36
CS-2019-93	FLR 1.25	0.543	OraPicoProk	9458 ± 55.4	527 ± 3.45
CS-2019-93	FLR 1.5	0.544	OraPicoProk	9399 ± 152	99 ± 2.75
CS-2019-93	FLR 2	0.543	OraPicoProk	9564 ± 128.4	63 ± 1.04

Note: Analyzed samples are from the Bay of Marseille for the first instrument and the coastal French waters of the Eastern English Channel Sea for the second one, generating different abundances for the same PFG. RedPicoProk are not expected in study area of instrument CS-2019-93.

The following experiment was conducted on CS-2015-68, using surface water collected at the SSL@MM point. Samples were selected to ensure the presence of RedPicoProk, such as after an upwelling [41]. A series of blanks were performed using a range between FLR 5 and 8 mV as a threshold, with PMTs on the "Medium" preset. "Non-phytoplankton events" generated when the sheath flows without a sample, as baseline of the instrument, were only observed for FLR 5 mV (Figure S2a) and 6 mV (Figure S2b); no events were recorded above the latter trigger threshold.

The resulting event rates at the FLR 5 mV trigger level reaches 10^4 events s^{-1} (Figure S2), exceeding the value when coincidence starts to affect counting by 10%, while it was 50 events s^{-1} at the FLR 6 mV trigger level. Optimized trigger exploration should be considered in parallel to coincidence. Conversely, no events were detected at FLR 7 and 8 mV. This suggests that FLR 6 mV was likely the most appropriate trigger level using PMT set to "Medium", the following experiments have confirmed this initial hypothesis.

3.2.2.1.2 | Step 2: Determining the Lowest FLR Trigger Threshold in a Natural Sample. Analyzing a natural sample generates additional "non-phytoplankton events", first because of the intercept between the laser and the sample core, and because the signatures of non-fluorescing particles emitted by their scattering still end up with unwanted signals in fluorescence on PMTs. The signature of these events must be included in the selection of the trigger threshold.

In this study, measurements were performed for each tested trigger level for 3 min at a pump speed of 3 $\mu L s^{-1}$. This experiment was conducted on two of the three described instruments (Table 1), each on natural seawater collected in the coastal area of its laboratory of origin. Data files were then processed using the CytoClus software, and particles were manually classified into phytoplankton and non-phytoplankton groups (as described in Section 2.2).

Concerning CS-2015-68 and following blank measurements presented in the previous section, trigger levels around the range previously tested were run: FLR 5, 6, 7, 8, 9, 11 and 12 mV. Trigger values above 7 mV were run for illustration purposes, as the blank measurements indicate the expected optimal trigger threshold above 5 and below 7 mV. Increasing the red fluorescence trigger threshold allows the "non-phytoplankton events" signature to gradually decrease, while minimizing their impact on the event rate, until the counts of smaller and dimmer particles (i.e RedPicoProk and OraPicoProk) are maximal (Table 2) and best distinguished from the "non-phytoplankton events" (Figure 3).

In this case study, based on natural samples collected at the SSL@MM, the smallest and dimmest fluorescing cells belonging to the RedPicoProk are highlighted (in magenta, Figure 3), and best visualized on the Max SWS versus Max FLR cytogram. Triggering on FLR 7 mV removes much of the "non-phytoplankton events" within "events smaller than 1 μm beads". However, it does not record the signal of all the smallest cells, particularly RedPicoProk, which shows a significant decrease in abundance (Table 2). Conversely, if the trigger threshold is too low (FLR $\leq$ 5 mV in our example), it produces an event rate exceeding the 10% difference caused by coincidence in this instrument, with few to no target phytoplankton cells counted, as shown in Table 2.

On older instruments, such as the one used for trigger optimization (CS-2015-68), if there are too many particles, leading to coincidence and computing limits, the analyzed volume will be significantly lower than the pumped volume. However, when using more recent ones, such as CS-2019-93, computing limits are reduced, PMT electronic noise levels are $\leq$ 1 mV,

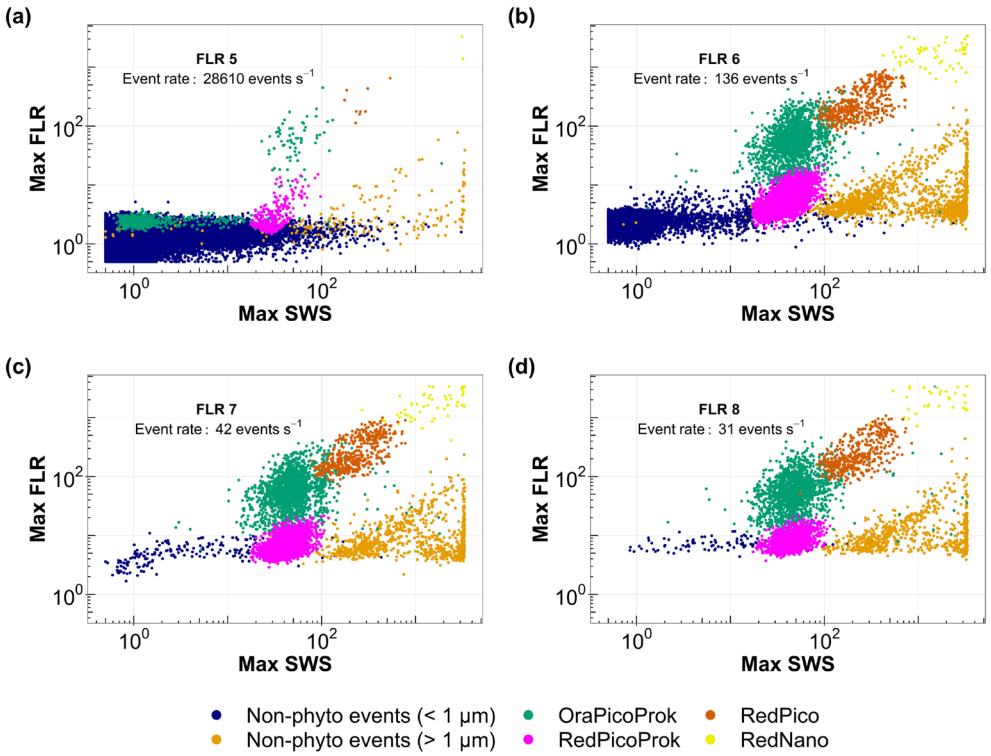

FIGURE 3 | Different trigger thresholds on a natural sample from the Bay of Marseille analyzed with instrument CS-2015-68, illustrated using Max FLR versus Max SWS cytograms. (a) FLR 5 mV, (b) FLR 6 mV, (c) FLR 7 mV, (d) FLR 8 mV under PMT preset to "Medium". Limit of 1 µm has been set on the Total FWS signal of 1 µm Silica beads (not shown), explaining the overlap among "non-phytoplankton events" groups. Measurement conditions (pump speed and measurement time) are identical between each tested trigger level. Groups are identified based on the recommended standard vocabulary and list of groups described in Section 2.2. [Color figure can be viewed at wileyonlinelibrary.com]

and analyzed volume (and thus cell abundance) is more stable as shown in Table 2. Illustration of the events can be found in Figure S3.

Concerning CS-2019-93, coincidence was not observed for event rates up to 5000 events s^{-1} (data not shown), trigger threshold between 1, 1.25, 1.5 and 2 mV generated the same counts for the OraPicoProk group while having an event rate decreasing from 3780 to 63 events s^{-1} (Table 2). As no RedPicoProk are expected in the English Channel Sea, all four triggers are suitable (Figure S3). However, to optimally record the dimmest particles from this instrument, a higher event rate increases both the noise-to-signal ratio and the coincidence probability, making FLR 1.25 mV a balanced compromise.

3.2.2.1.3 | Step 3: Determining the Lowest SWS Trigger Threshold. Scatter is used for size conversion with a set of beads of known size as a reference, but it may also benefit from images collected simultaneously from targeted cells ([17, 52–54]). Triggering on the SWS ensures the recording of the entire pulse shape, which may not be the case when triggering on FLR, especially for large particles. If the trigger for data acquisition is set on FLR, the instrument will begin data acquisition for all the optical parameters only when the red fluorescence reaches the threshold level. If the pigments are not evenly spread in the cells, the light scattered by the area of the cell without chlorophyll will not be recorded. If SWS or FWS pulse shapes are not fully recorded, the length estimates of larger particles, based on their time of flight from the start of recording, will be affected. Example of images recorded simultaneously with their pulse shapes in samples collected at the SSL@MM station, triggered either on FLR or on SWS using the CS-2015-68, are illustrated on Figure 4.

Figure 4a,b demonstrates the discrepancy between the estimated size on a picture taken when triggering on the FLR, reaching approximately (a) 180 µm (Figure 4a) and 90 µm (Figure 4b); and the signal length of the pulse shape, approximately (a) 60 µm (Figure 4a) and 50 µm (Figure 4b). On the other hand, the pulse shape length recorded while triggering on SWS is similar to the size measured in the picture (Figure 4c). However, this should not affect particles smaller than 10 µm as morphological features are scarce and cells are mostly round shaped and filled homogeneously with chloroplasts, meaning the FWS and SWS pulse shapes are superimposed on the fluorescence pulse shapes. When implementing a protocol that triggers on SWS, it is still a prerequisite to first establish the lower limits for a FLR trigger before optimizing the SWS trigger threshold. This step ensures that small and dim communities are not overlooked, particularly in unknown environments.

Independently from the trigger source (FLR or SWS) or threshold, large particles with high pigment content will produce truncated optical pulse shapes, as they reach the maximum capacity of PMT conversion, as illustrated in Figure 5. Therefore, using the area under the curve to measure a particle's total signal can underestimate the contribution of larger cells, such as microphytoplankton, when converting pulse shapes into size and pigment content. Additionally, large cells may not align with the flow or

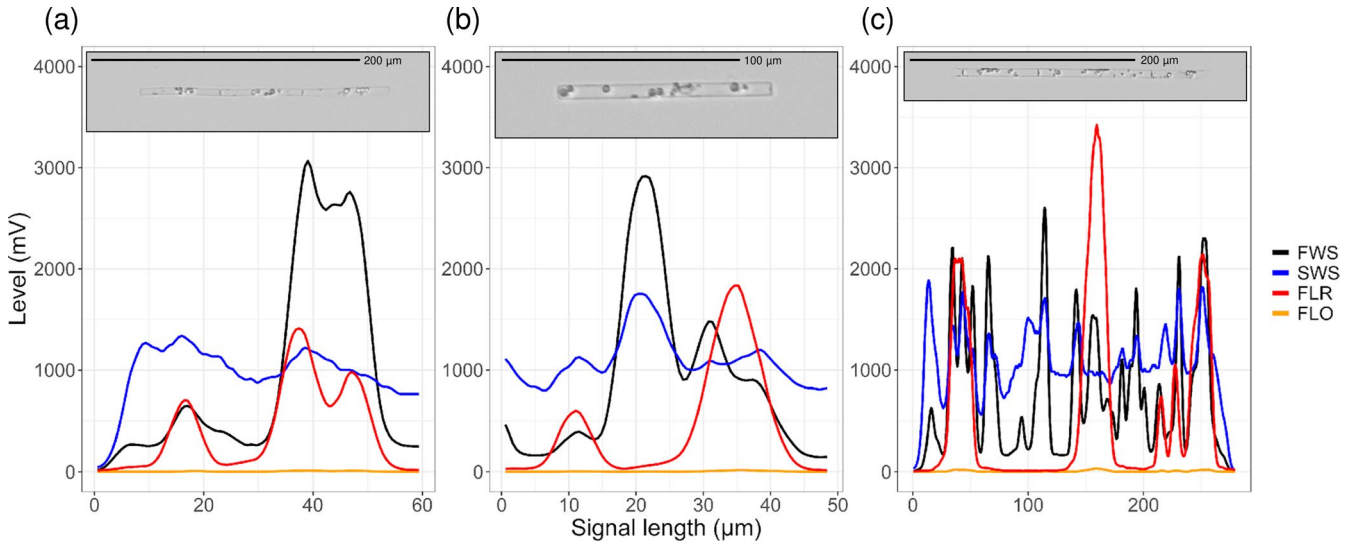

FIGURE 4 | Effect of triggering on FLR (FLR 25 mV, a and b) and triggering on SWS (SWS 150 mV, c) demonstrating the discrepancy between the size estimated from images and that from pulse shapes (example collected on the CS-2015-68). PMT voltage was set to "Medium". *In the case of chain-forming cells, the entire chain is treated as a single particle and appears as a single point on a 2D cytogram. Only pulse shapes and images allow the signals of individual cells within the chain to be distinguished.* [Color figure can be viewed at wileyonlinelibrary.com]

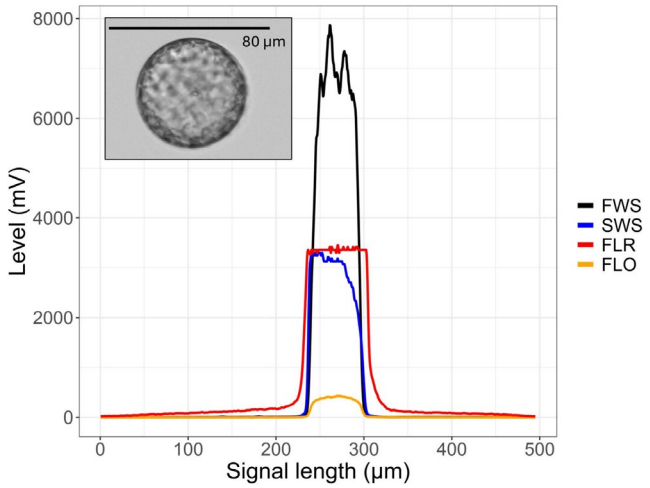

FIGURE 5 | Effect on the pulse shape of a diatom when PMT saturation by red photons generates a plateau at around 3300 mV (CS-2015-68). Trigger level was set to FLR 25 mV and PMT voltage to "Medium". [Color figure can be viewed at wileyonlinelibrary.com]

may show morphological complex features, generating pulse shapes that are not related to size.

3.2.2.2 | PMT Voltage Optimization. In the previous section, the trigger thresholds on FLR or SWS channels were optimized to detect the dimmest fluorescing cells, using a fixed PMT voltage preset to "Medium".

Increasing the PMT voltage enhances the gain, improving the separation between dimly fluorescing or scattering particles and "non-phytoplankton events", up to a certain point depending on the type of PMT. However, raising the PMT voltage while maintaining the previously optimized low trigger threshold results in increased "non-phytoplankton event" signal. Therefore, if PMT voltages are modified after setting the trigger threshold, the trigger optimization process must be repeated.

Samples for this experiment were collected at 50m depth at the SOMLIT station, to ensure the presence of highly fluorescing RedPicoProk. Measurements were acquired for each tested trigger level and PMT settings for three minutes at a pump speed of $3\,\mu L\,s^{-1}$. Data files were then processed using CytoClus 5 software, and particles were manually classified into phytoplankton and non-phytoplankton groups (as described in Section 2.2). Range of trigger levels were based on the findings of the previous section. For PMT preset to "Medium", trigger levels were run on a range from FLR 5 to 8 mV. For PMT preset to "Low", trigger levels were run on a range from FLR 3–8 mV. For PMT preset to "High", trigger levels were run on a range from FLR 5 to 12 mV.

While maintaining low coincidence, results indicate that maximal estimated abundances of the RedPicoProk group are collected at PMT "Medium" – trigger threshold FLR 6 mV and at PMT "High" – trigger threshold FLR 9 mV (Figure S4). Indeed, abundances were respectively 39,890 and 39,610 cells mL^{-1}. The other settings either removed the baseline corresponding to "non-phytoplankton events", or were above the coincidence level of 10% difference with expected counts. Some trigger levels are not shown in Figure S4, because the corresponding acquisition resulted in empty files due to high event rates (i.e., PMT "Low", and FLR trigger thresholds 3 and 4 mV and PMT "High" – FLR trigger thresholds 5, 6, 7 mV).

When applying multiple protocols to a single sample, it is recommended to maintain consistent PMT levels across runs to facilitate data comparison and ensure consistent analytical outcomes. In the case of using combined protocols with different trigger thresholds to resolve the entire community, changing PMT gains between them will change the fluorescence or scatter references. This will change the position of similar groups

on cytograms and may complicate group recognition in between acquisition protocols and automated classification methods [53].

4 | Discussion

The goal of best practices on data acquisition is to generate easily interoperable data between users despite the diversity of CytoSense-type flow cytometers and their configurations, as used in aquatic microbiology. It leads to a better assessment of trends and patterns in microbial ecology on broader temporal and spatial scales. After establishing a recommended standardized vocabulary [38], it is essential to share and apply standardized common protocols to reach the optimal flow cytometer configuration for accurately characterizing phytoplankton populations, functional traits and cell properties. These are essential to consistently determine flow cytometric plankton functional groups (PFG) and build training sets for automated analysis [53]. Ultimately, they contribute to building new databases following the FAIRness principle (Findability, Accessibility, Interoperability, and Reuse of digital assets) required for reliable environmental policy and management [55].

4.1 | Configuring Optimal Settings

When analyzing a sample to characterize phytoplankton, "non-phytoplankton events" consist of a mix of optical and electronic noise and non-targeted particles, ranging from submicron to several hundreds of micrometers (e.g., viruses, grazers or detritus). "Non-phytoplankton events" should not affect the accurate collection of phytoplankton cells in terms of resolution and counting. From a blank measurement, "events smaller than 1 μm beads" that are not phytoplankton were extracted but did not give the full baseline of events generated by the sample core and non-fluorescing particles. Additional "non-phytoplankton events", such as signal from non-autofluorescing particles (detritus, heterotrophic cells, viruses) or the scatter between the sheath and the sample core, can only be identified when analyzing a natural sample. Larger "non-phytoplankton events", such as grazers and large detritus usually bear signatures much lower in FLR compared to phytoplankton groups.

This baseline of "non-phytoplankton events" can represent a significant proportion of the total acquisition (Figure 6), but will affect phytoplankton counts if coincidence increases, this was the case for FLR 5 mV (Figure 6a) and FLR 1 mV (Figure 6b), with PMTs set to "Medium". Conversely, this baseline should not be completely eliminated to ensure that the smallest/dimmest groups are not truncated. In our case, FLR 7 mV shows a higher proportion of phytoplankton events relative to the total, but fails to accurately resolve smaller/dimmer phytoplankton groups (Figure 6a).

As such, in this study, RedPicoProk cells, probably belonging to *Prochlorococcus*, overlap with the submicron "non-phytoplankton events". Cytograms from Figure 3 highlight the importance of lowering trigger levels but also acquiring a certain amount of "events smaller than 1 μm beads" to adequately capture the smallest and dimmest auto-fluorescing groups in the samples. They also show the possibility of confusing "non-phytoplankton events" signals with live organisms. Up to a certain point, adjusting the PMT voltage can improve signal separation, though the extent of improvement depends on the type of PMTs and the laser power.

As such, a 125 mW–488 nm is a good compromise for RedPicoProk resolution, but setting PMTs to "High" may generate considerable noise. This may not occur as drastically with a 60 mW laser. However, a 60 mW laser power would not be efficient to resolve

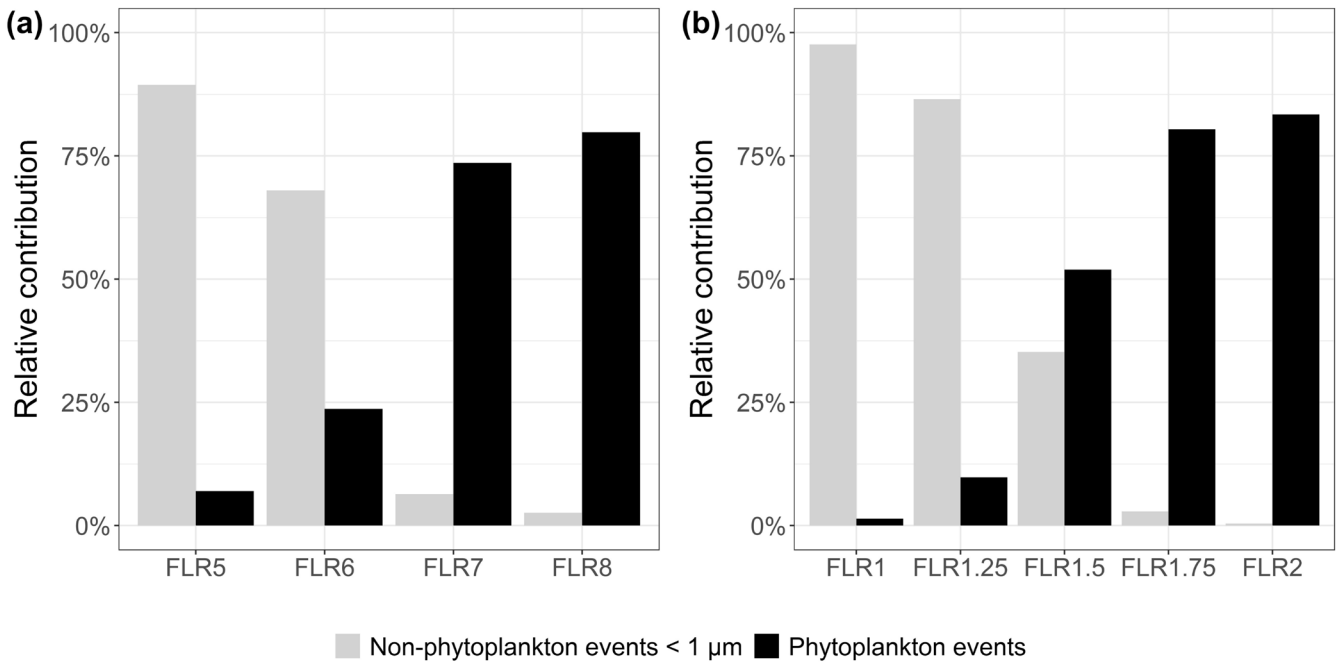

FIGURE 6 | Proportion of phytoplankton cells (black) compared to "non-phytoplankton events", more precisely, the "events smaller than 1 μm beads" (grey) depending on different trigger levels (mV) with PMT preset to "Medium" for instruments (a) CS-2015-68 and (b) CS-2019-93. Missing values correspond to "non-phytoplankton events" more specifically "events larger than 1 μm beads".

the RedPicoProk group. Concerning PMT voltage optimization on CS-2015-68, similar abundances for RedPicoProk cells were evidenced between PMT "Medium" – trigger FLR 6mV and PMT "High" – trigger FLR 9 mV (Figure S4). However, "High" PMT voltage combined with a high-power laser accelerates the saturation of the pulse shapes, reducing the resolution of the maximum values of the signal. This is visible on Figure S4k,l, where RedNano and RedMicro cells are positioned on an upper left corner of the cytogram. In this case, it would thus be recommended to opt for "Medium" PMT voltage over "High", to limit saturation. At PMT "Low" trigger FLR 4 mV, computational limits may have been reached by the noise, resulting in empty files. At FLR 5 mV, RedPicoProk cells seem to be underestimated, as the highest abundances for PMT "Low" is approximately 3 times lower compared to PMT "Medium" and "High". This likely reflects the system operating at the edge of FLR trigger sensitivity and PMT detection capabilities, as OraPicoProk counts are similar to PMT "Medium", FLR trigger 6 mV.

In areas where the smallest cells are OraPicoProk, the optimization procedure should be the same, e.g., a compromise between event rate of non-targeted particles and resolution of phytoplankton. For instance, instrument CS-2019-93 which has improved in computing speed compared to CS-2015-68, accurately counts OraPicoProk while increasing "non-phytoplankton events". The baseline did not change in between trigger FLR 1 and 1.25 mV, but signal over noise changed from less than 1% to ~10% (Figure 6b), suggesting the 1.25 mV value to optimize counting of phytoplankton cells while limiting coincidence.

4.2 | Additional Considerations

4.2.1 | Acquisition Protocols for Optimal Community Resolution: Integrating Small, Abundant Groups With Large, Rare Ones

Flow cytometers such as the CytoSense can run larger volumes than conventional flow cytometers (up to several mL). A compromise is therefore necessary to handle the wide range of optical characteristics – from small, dim but abundant picophytoplankton to the large, highly fluorescent, but scarce microphytoplankton [18, 22, 26, 56].

To address this, one approach is to run two distinct protocols per sample, one dedicated to very abundant picophytoplankton, with a low analyzed volume (0.3-1 mL, depending on the available time and volume), using the lowest optimal trigger threshold on FLR. This first protocol will be the same as the optimized protocol from Section 3.2.2. Another protocol can be set, dedicated to less abundant nanophytoplankton and microphytoplankton with increased trigger threshold, to filter out the small cells and increase the volume acquired (5-10 mL depending on available time and volume). In the latter, an additional SWS trigger can be used to record pulse shapes in their entirety and obtain an accurate particle length estimation. This second protocol uses the picophytoplankton groups identified in the first protocol as reference to define the trigger threshold. Running one acquisition aiming to resolve the full size-classes can be done if the instrument's computer can manage data-heavy files [17, 57].

4.2.2 | Instrument Temperature

Field-deployed automated instruments experience wide temperature fluctuations, impacting cytometer function by altering sheath/sample viscosity and potentially affecting electronics [13]. During a May 2015 deployment on RV *Simon Stevin* in the North Sea, instrument CS-2013-51 overheated [58]. Calibration beads (3.0 µm Cyto-Cal 488 nm, Duke Scientific) tracked laser stability, revealing changes in optical intensities with rising sheath, PMT, and laser temperatures (18°C–35°C; data not shown). Regular bead analysis showed increasing system temperature resulted in reduced red, yellow and orange maximum fluorescence [58]. Though unreplicated, this study strongly recommends using temperature-controlled rooms when possible (below 25°C) or correcting pulse shape biases in data analysis.

4.2.3 | Using Beads for Stability Monitoring and Optical Unit Normalization

Using two sizes of fluorescing beads for instrument monitoring is recommended to avoid creating a bias in case one of the bead solutions starts to decay. Furthermore, to convert fluorescence into pigment units by comparing it with in vivo chlorophyll *a* [54, 59, 60] or size [17], phytoplankton groups need to be normalized to one of the two sets of beads, depending on their size. A set of beads of different sizes and fluorescence has to be analyzed after any realignment or changes in optical settings, in addition to the stability as described in a previous section.

5 | Conclusion

Given the need for global datasets [61], interoperability must be a central focus in aquatic flow cytometry. The presented best practices aim to optimize acquisitions by determining the limits of CytoSense instruments, producing cytograms that are easy to analyze and ensuring interoperable datasets.

Optimizing the trigger threshold and the PMT voltage is an interactive process. To determine the best settings, the signature of "non-phytoplankton events" should be used as a reference line. Combined with the event rate and the highest estimated abundances, optimal configurations can be assessed. However, an optimized instrument does not necessarily measure all the targeted particles nor prevent from over-counting due to overlapping dim fluorescing cells with "non-phytoplankton events"; rather, it indicates that the user has determined the instrument's optimal conditions for measurement. Keeping in mind the aforementioned best practices, this article provides a summary of recommendations in Table S1.

This work was based on the consultation of a consortium of automated and benchtop flow cytometry experts to collect, gather and experiment the main considerations when using CytoSense-type instruments in aquatic environments. This was most notably conducted in the preparation and execution of the EuroMarine TT – Cyto workshop in June 2024, for which the presentations are publicly available [62–66].

Author Contributions

Clémentine Gallot: conceptualization, methodology, data curation, investigation, validation, formal analysis, visualization, writing – original draft, writing – review and editing. **Zéline Hubert:** conceptualization, methodology, data curation, investigation, validation, formal analysis, visualization, writing – original draft, writing – review and editing. **Lumi Haraguchi:** conceptualization, methodology, investigation, data curation, validation, funding acquisition, project administration, resources, writing – original draft, writing – review and editing. **Hedy Aardema:** conceptualization, validation, writing – review and editing. **Luis Felipe Artigas:** conceptualization, methodology, validation, funding acquisition, project administration, resources, writing – review and editing. **Amel Bellaaj Zouari:** conceptualization, validation, writing – review and editing. **Arnaud Cauvin:** conceptualization, investigation, validation, writing – review and editing. **Raffaella Casotti:** conceptualization, validation, funding acquisition, writing – review and editing. **Véronique Créach:** conceptualization, validation, funding acquisition, project administration, writing – review and editing. **Georges Dubelaar:** conceptualization, validation, writing – review and editing. **Alexandre Epinoux:** conceptualization, validation, writing – review and editing. **Gérald Grégori:** conceptualization, methodology, validation, funding acquisition, writing – review and editing. **Oliver Grosso:** conceptualization, validation, writing – review and editing. **Joanna Kolasinki:** conceptualization, validation, writing – review and editing. **Harrie Kools:** conceptualization, methodology, validation, writing – review and editing. **Rob Lievaart:** conceptualization, validation, writing – review and editing. **Arnaud P. Louchart:** conceptualization, methodology, validation, formal analysis, visualization, writing – review and editing. **Glaucia Moreira Fragoso:** conceptualization, validation, writing – review and editing. **Maialen Palazot:** conceptualization, investigation, validation, writing – review and editing. **Machteld Rijkeboer:** conceptualization, methodology, investigation, formal analysis, validation, writing – review and editing. **Kévin Robache:** conceptualization, validation, visualization, writing – review and editing. **Joseph Rolland:** conceptualization, methodology, data curation, investigation, validation, visualization, writing – original draft, writing – review and editing. **Thomas Rutten:** conceptualization, validation, writing – review and editing. **Melilotus Thyssen:** conceptualization, methodology, investigation, validation, formal analysis, supervision, funding acquisition, project administration, resources, writing – original draft, writing – review and editing.

Acknowledgments

The authors would like to thank the participants of the EuroMarine TT-cyto workshop held in June 2024 in Wimereux (France), for participating in constructive discussions that lead to drafting this Best Practices for Phytoplankton Analysis with CytoSense flow cytometers reference document. The authors thank the SSL@MM (SeaWater Sensing Laboratory@MIO Marseille) facility, Michel Durand, the divers of OSU PYTHEAS, the French National Littoral Ecosystems Observation System (SOMLIT) funded by the French Littoral and Coastal Research Infrastructure IR ILICO, the Antédon mission boat, Aix Marseille University, CNRS and A*MIDEX, a French "Investissements d'Avenir" program. They dedicate special thanks to the EuroMarine consortium for their help in sustaining the TT-Cyto Workshop and the manuscript redaction and publishing, in addition to European Commission's *H2020*-INFRAIA (2019-1 n° 871153 and 951799), European Commission's Horizon 2020 Research and Innovation program (101081642), French Prioritary Research Project RiOMar (ProjetIA-22-POCE-0006) and IFSea Graduate School (ANR-21-EXES-00 11), as well as LOG and ISML ULCO hosting the TT-Cyto Workshop. Authors would also like to thank the crew of the research vessel Sepia II (French Oceanographic Fleet – FOF) and IFREMER COAST LER/BL for the collection of samples off Boulogne-sur-Mer. Technical support and equipment funds were provided by French State and "Hauts-de-France" region frame contract projects MARCO and IDEAL, as well as by the EU Marine Strategy Framework Directive, n2101893310 for assessing the monitoring program of pelagic habitats for the Marine Strategy Framework Directive (MSFD). Z.H. was supported by a "Hauts-de-France" regional Doctorate and ULCO doctorate research grant and a CNRS engineer contract. The authors would like to thank Sami Kielosto for the support deploying the instrument on board M/S Finnmaid. This study utilized research infrastructure as part of FINMARI (Finnish Marine Research Infrastructure consortium).

The following proprietary products are mentioned for methodological clarity: CytoSense and CytoBuoy flow cytometers, CytoUSB and CytoClus software (CytoBuoy b.v.), Fluoresbrite microspheres (Polysciences), FluoSpheres (Thermo Fisher Scientific), Rainbow Fluorescent Particles (BioLegend), and Proclin preservative (Sigma-Aldrich). Mention of trade names does not constitute endorsement.

Conflicts of Interest

The authors declare no conflicts of interest.

Data Availability Statement

Data concerning the experiments are available on https://www.seanoe.org/data/00935/104684/.

References

1. H. M. Shapiro, *Practical Flow Cytometry* (John Wiley and Sons, 2003).

2. A. S. Paau, J. Oro, and J. R. Cowles, "Application of Flow Microflorometry to the Study of Algal Cells and Isolated Chloroplasts," *Journal of Experimental Botany* 29, no. 4 (1978): 1011–1020, https://doi.org/10.1093/jxb/29.4.1011.

3. C. M. Yentsch and C. S. Yentsch, "Emergence of Optical Instrumentation for Measuring Biological Properties," in *Oceanography and Marine Biology, an Annual Review*, vol. 22 (CRC Press, 1984), 47.

4. C. Courties, A. Vaquer, M. Troussellier, et al., "Smallest Eukaryotic Organism," *Nature* 370, no. 6487 (1994): 255, https://doi.org/10.1038/370255a0.

5. W. K. W. Li, D. V. S. Rao, W. G. Harrison, et al., "Autotrophic Picoplankton in the Tropical Ocean," *Science* 219, no. 4582 (1983): 292–295, https://doi.org/10.1126/science.219.4582.292.

6. A. Martin, "Phytoplankton Patchiness: The Role of Lateral Stirring and Mixing," *Progress in Oceanography* 57 (2003): 125–174, https://doi.org/10.1016/S0079-6611(03)00085-5.

7. R. J. Olson, D. Vaulot, and S. W. Chisholm, "Marine Phytoplankton Distributions Measured Using Shipboard Flow Cytometry," *Deep Sea Research Part A. Oceanographic Research Papers* 32, no. 10 (1985): 1273–1280, https://doi.org/10.1016/0198-0149(85)90009-3.

8. M. Troussellier, C. Courties, and A. Vaquer, "Recent Applications of Flow Cytometry in Aquatic Microbial Ecology," *Biology of the Cell* 78, no. 1–2 (1993): 111–121, https://doi.org/10.1016/0248-4900(93)90121-T.

9. G. M. Fragoso, A. J. Poulton, N. J. Pratt, G. Johnsen, and D. A. Purdie, "Trait-Based Analysis of Subpolar North Atlantic Phytoplankton and Plastidic Ciliate Communities Using Automated Flow Cytometer," *Limnology and Oceanography* 64, no. 4 (2019): 1763–1778, https://doi.org/10.1002/lno.11189.

10. F. Pomati, N. J. B. Kraft, T. Posch, B. Eugster, J. Jokela, and B. W. Ibelings, "Individual Cell Based Traits Obtained by Scanning Flow-Cytometry Show Selection by Biotic and Abiotic Environmental Factors During a Phytoplankton Spring Bloom," *PLoS One* 8, no. 8 (2013): e71677, https://doi.org/10.1371/journal.pone.0071677.

11. S. Jacquet, J.-F. Lennon, and D. Vaulot, "Application of a Compact Automatic Sea Water Sampler to High Frequency Picoplankton Studies," *Aquatic Microbial Ecology* 14, no. 3 (1998): 309–314, https://doi.org/10.3354/ame014309.

12. H. Sosik, R. Olson, M. Neubert, A. Shalapyonok, and A. Solow, "Growth Rates of Coastal Phytoplankton From Time-Series Measurements With a Submersible Flow Cytometer," *Limnology and Oceanography* 48, no. 5 (2003): 1756–1765, https://doi.org/10.4319/lo.2003.48.5.1756.

13. G. B. J. Dubelaar, P. L. Gerritzen, A. E. R. Beeker, R. R. Jonker, and K. Tangen, "Design and First Results of CytoBuoy: A Wireless Flow Cytometer for In Situ Analysis of Marine and Fresh Waters," *Cytometry* 37, no. 4 (1999): 247–254, https://doi.org/10.1002/(SICI)1097-0320(19991201)37:4<247::AID-CYTO1>3.0.CO;2-9.

14. R. J. Olson, A. Shalapyonok, and H. M. Sosik, "An Automated Submersible Flow Cytometer for Analyzing Pico- and Nanophytoplankton: FlowCytobot," *Deep-Sea Research Part I: Oceanographic Research Papers* 50, no. 2 (2003): 301–315, https://doi.org/10.1016/S0967-0637(03)00003-7.

15. F. Ribalet, D. M. Schruth, and E. V. Armbrust, "flowPhyto: Enabling Automated Analysis of Microscopic Algae From Continuous Flow Cytometric Data," *Bioinformatics* 27, no. 5 (2011): 732–733, https://doi.org/10.1093/bioinformatics/btr003.

16. J. E. Swalwell, F. Ribalet, and E. V. Armbrust, "SeaFlow: A Novel Underway Flow-Cytometer for Continuous Observations of Phytoplankton in the Ocean," *Limnology and Oceanography: Methods* 9, no. 9 (2011): 466–477, https://doi.org/10.4319/lom.2011.9.466.

17. M. Dugenne, M. Thyssen, D. Nerini, et al., "Consequence of a Sudden Wind Event on the Dynamics of a Coastal Phytoplankton Community: An Insight Into Specific Population Growth Rates Using a Single Cell High Frequency Approach," *Frontiers in Microbiology* 5 (2014): 485, https://doi.org/10.3389/fmicb.2014.00485.

18. Z. Hubert, A. P. Louchart, K. Robache, et al., "Decadal Changes in Phytoplankton Functional Composition in the Eastern English Channel: Possible Upcoming Major Effects of Climate Change," *Ocean Science* 21 (2025): 679–700, https://doi.org/10.5194/os-21-679-2025.

19. K. Robache, Z. Hubert, C. Gallot, et al., "Multi-Scale Phytoplankton Dynamics in a Coastal System of the Eastern English Channel: The Boulogne-Sur-Mer Coastal Area," *Ocean Science* 21, no. 4 (2025): 1787–1811, https://doi.org/10.5194/os-21-1787-2025.

20. M. Thyssen, G. A. Tarran, M. V. Zubkov, et al., "The Emergence of Automated High-Frequency Flow Cytometry: Revealing Temporal and Spatial Phytoplankton Variability," *Journal of Plankton Research* 30, no. 3 (2008): 333–343, https://doi.org/10.1093/plankt/fbn005.

21. S. Bonato, U. Christaki, A. Lefebvre, F. Lizon, M. Thyssen, and L. F. Artigas, "High Spatial Variability of Phytoplankton Assessed by Flow Cytometry, in a Dynamic Productive Coastal Area, in Spring: The Eastern English Channel," *Estuarine, Coastal and Shelf Science* 154 (2015): 214–223, https://doi.org/10.1016/j.ecss.2014.12.037.

22. P. Marrec, G. Grégori, A. M. Doglioli, et al., "Coupling Physics and Biogeochemistry Thanks to High-Resolution Observations of the Phytoplankton Community Structure in the Northwestern Mediterranean Sea," *Biogeosciences* 15, no. 5 (2018): 1579–1606, https://doi.org/10.5194/bg-15-1579-2018.

23. R. Tzortzis, A. M. Doglioli, S. Barrillon, et al., "Impact of Moderately Energetic Fine-Scale Dynamics on the Phytoplankton Community Structure in the Western Mediterranean Sea," *Biogeosciences* 18, no. 24 (2021): 6455–6477, https://doi.org/10.5194/bg-18-6455-2021.

24. R. Tzortzis, A. M. Doglioli, M. Messié, et al., "The Contrasted Phytoplankton Dynamics Across a Frontal System in the Southwestern Mediterranean Sea," *Biogeosciences* 20, no. 16 (2023): 3491–3508, https://doi.org/10.5194/bg-20-3491-2023.

25. L. Serre-Fredj, F. Jacqueline, M. Navon, et al., "Coupling High Frequency Monitoring and Bioassay Experiments to Investigate a Harmful Algal Bloom in the Bay of Seine (French-English Channel)," *Marine Pollution Bulletin* 168 (2021): 112387, https://doi.org/10.1016/j.marpolbul.2021.112387.

26. I. Boudriga, M. Abdennadher, Y. Khammeri, et al., "Karenia Selliformis Bloom Dynamics and Growth Rate Estimation in the Sfax Harbour (Tunisia), by Using Automated Flow Cytometry Equipped With Image in Flow, During Autumn 2019," *Harmful Algae* 121 (2023): 102366, https://doi.org/10.1016/j.hal.2022.102366.

27. A. Louchart, F. Lizon, E. Debusschere, et al., "The Importance of Niches in Defining Phytoplankton Functional Beta Diversity During a Spring Bloom," *Marine Biology* 171, no. 1 (2024): 26, https://doi.org/10.1007/s00227-023-04346-6.

28. L. Berline, A. M. Doglioli, A. Petrenko, et al., "Long-Distance Particle Transport to the Central Ionian Sea," *Biogeosciences* 18, no. 24 (2021): 6377–6392, https://doi.org/10.5194/bg-18-6377-2021.

29. I. Boudriga, C. Poindron, Y. Khammeri, et al., "Impact of Atmospheric Deposition on the Dynamics of Ultraphytoplanktonic Populations in the Gulf of Gabès During an Intense Dust Event (MERITE-HIPPOCAMPE Campaign)," *Marine Pollution Bulletin* 200 (2024): 116059, https://doi.org/10.1016/j.marpolbul.2024.116059.

30. M. Vannoni, A. Grant, D. Sheahan, and V. Créach, "Evaluating the Impact of Residual Low Chlorine Concentration on Phytoplankton Communities by Flow Cytometry," *Chemosphere* 367 (2024): 143634, https://doi.org/10.1016/j.chemosphere.2024.143634.

31. S. W. Chisholm, R. J. Olson, E. R. Zettler, R. Goericke, J. B. Waterbury, and N. A. Welschmeyer, "A Novel Free-Living Prochlorophyte Abundant in the Oceanic Euphotic Zone," *Nature* 334, no. 6180 (1988): 340–343, https://doi.org/10.1038/334340a0.

32. H. T. Maecker and J. Trotter, "Flow Cytometry Controls, Instrument Setup, and the Determination of Positivity," *Cytometry, Part A* 69A, no. 9 (2006): 1037–1042, https://doi.org/10.1002/cyto.a.20333.

33. E. Sliwinska, J. Loureiro, I. J. Leitch, et al., "Application-Based Guidelines for Best Practices in Plant Flow Cytometry," *Cytometry, Part A* 101, no. 9 (2022): 749–781, https://doi.org/10.1002/cyto.a.24499.

34. J. M. Gasol and P. A. del Giorgio, "Using Flow Cytometry for Counting Natural Planktonic Bacteria and Understanding the Structure of Planktonic Bacterial Communities," *Scientia Marina* 64, no. 2 (2000): 197–224, https://doi.org/10.3989/scimar.2000.64n2197.

35. D. Marie, N. Simon, and D. Vaulot, "Phytoplankton Cell Counting by Flow Cytometry," in *Algal Culturing Techniques* (Elsevier, 2005).

36. M. C. Pernice and J. M. Gasol, "Automated Flow Cytometry as a Tool to Obtain a Fine-Grain Picture of Marine Prokaryote Community Structure Along an Entire Oceanographic Cruise," *Frontiers in Microbiology* 13 (2023): 1064112, https://doi.org/10.3389/fmicb.2022.1064112.

37. M. J. W. Veldhuis and G. W. Kraay, "Application of Flow Cytometry in Marine Phytoplankton Research: Current Applications and Future Perspectives," *Scientia Marina* 64, no. 2 (2000): 121–134, https://doi.org/10.3989/scimar.2000.64n2121.

38. M. Thyssen, G. Grégori, V. Créach, et al., "Interoperable Vocabulary for Marine Microbial Flow Cytometry," *Frontiers in Marine Science* 9 (2022): 975877, https://doi.org/10.3389/fmars.2022.975877.

39. A. Neeley, I. Soto, and C. Proctor, *Standards and Best Practices for Reporting Flow Cytometry Observations: A Technical Manual. Version 1.1* (NASA Goddard Space Flight Center, 2023), https://doi.org/10.25607/OBP-1864.2.

40. X. Durrieu de Madron, C. Guieu, R. Sempéré, et al., "Marine Ecosystems' Responses to Climatic and Anthropogenic Forcings in the Mediterranean," *Progress in Oceanography* 91, no. 2 (2011): 97–166, https://doi.org/10.1016/j.pocean.2011.02.003.

41. R. Fuchs, V. Rossi, C. Caille, et al., "Intermittent Upwelling Events Trigger Delayed, Major, and Reproducible Pico-Nanophytoplankton Responses in Coastal Oligotrophic Waters," *Geophysical Research Letters* 50, no. 5 (2023): e2022GL102651, https://doi.org/10.1029/2022GL102651.

42. G. Grégori, A. Colosimo, and M. Denis, "Phytoplankton Group Dynamics in the Bay of Marseilles During a 2-Year Survey Based on Analytical Flow Cytometry," *Cytometry* 44, no. 3 (2001): 247–256, https://doi.org/10.1002/1097-0320(20010701)44:3<247::AID-CYTO1117>3.0.CO;2-Z.

43. Z. Hubert, A. Libeau, C. Gallot, et al., "Phytoplankton Coastal-Offshore Monitoring by the Strait of Dover at High Spatial Resolution: The DYPHYRAD Surveys [Preprint]," *Earth System Science Data Discussions* (2025), https://doi.org/10.5194/essd-2025-131.

44. J. M. Brylinski, Y. Lagadeuc, V. Gentilhomme, et al., "Le fleuve côtier: Un phénomène hydrologique important en Manche orientale. Exemple du Pas-de-Calais," *Oceanologica Acta* 11 (1991): 193–203.

45. A. Lefebvre, N. Guiselin, F. Barbet, and F. L. Artigas, "Long-Term Hydrological and Phytoplankton Monitoring (1992–2007) of Three Potentially Eutrophic Systems in the Eastern English Channel and the Southern Bight of the North Sea," *ICES Journal of Marine Science* 68, no. 10 (2011): 2029–2043, https://doi.org/10.1093/icesjms/fsr149.

46. M. Schapira, D. Vincent, V. Gentilhomme, and L. Seuront, "Temporal Patterns of Phytoplankton Assemblages, Size Spectra and Diversity During the Wane of a *Phaeocystis Globosa* Spring Bloom in Hydrologically Contrasted Coastal Waters," *Journal of the Marine Biological Association of the United Kingdom* 88, no. 4 (2008): 649–662, https://doi.org/10.1017/S0025315408001306.

47. D.-I. Skouroliakou, E. Breton, and U. Christaki, "And Diatom Blooms Promote Distinct Bacterial Communities and Associations in a Coastal Ecosystem," *Environmental Microbiology Reports* 16, no. 4 (2024): e13313, https://doi.org/10.1111/1758-2229.13313.

48. F. Partensky, W. R. Hess, and D. Vaulot, "Prochlorococcus, a Marine Photosynthetic Prokaryote of Global Significance," *Microbiology and Molecular Biology Reviews* 63, no. 1 (1999): 106–127, https://doi.org/10.1128/mmbr.63.1.106-127.1999.

49. D. Marie, F. Rigaut-Jalabert, and D. Vaulot, "An Improved Protocol for Flow Cytometry Analysis of Phytoplankton Cultures and Natural Samples," *Cytometry, Part A* 85, no. 11 (2014): 962–968, https://doi.org/10.1002/cyto.a.22517.

50. E. S. Chase and R. A. Hoffman, "Resolution of Dimly Fluorescent Particles: A Practical Measure of Fluorescence Sensitivity," *Cytometry* 33 (1998): 267–279, https://doi.org/10.1002/(SICI)1097-0320(19981001)33:2<267::AID-CYTO24>3.0.CO;2-R.

51. N. Jiao, T. Luo, R. Zhang, et al., "Presence of Prochlorococcus in the Aphotic Waters of the Western Pacific Ocean," *Biogeosciences* 11, no. 8 (2014): 2391–2400, https://doi.org/10.5194/bg-11-2391-2014.

52. L. Duforêt-Gaurier, C. Gallot, D. Schaffer, and M. Thyssen, "Comparison of Existing Methods to Derive Phytoplankton Cell Diameter From Flow Cytometry and Ways for Improvements," 2025.

53. R. Fuchs, M. Thyssen, V. Creach, et al., "Automatic Recognition of Flow Cytometric Phytoplankton Functional Groups Using Convolutional Neural Networks," *Limnology and Oceanography: Methods* 20, no. 7 (2022): 387–399, https://doi.org/10.1002/lom3.10493.

54. L. Haraguchi, H. H. Jakobsen, N. Lundholm, and J. Carstensen, "Monitoring Natural Phytoplankton Communities: A Comparison Between Traditional Methods and Pulse-Shape Recording Flow Cytometry," *Aquatic Microbial Ecology* 80, no. 1 (2017): 77–92, https://doi.org/10.3354/ame01842.

55. S. Lahbib, S. Claus, P. Oset, M. Fichaut, and M. Thyssen, *Ingesting, Validating, Long-Term Storage and Access of Flow Cytometer Data* (SeaDataCloud, 2019), https://repository.oceanbestpractices.org/handle/11329/1035.

56. M. Thyssen, G. J. Grégori, J.-M. Grisoni, et al., "Onset of the Spring Bloom in the Northwestern Mediterranean Sea: Influence of Environmental Pulse Events on the In Situ Hourly-Scale Dynamics of the Phytoplankton Community Structure," *Frontiers in Microbiology* 5 (2014): 1–16, https://doi.org/10.3389/fmicb.2014.00387.

57. S. Bonato, E. Breton, M. Didry, et al., "Spatio-Temporal Patterns in Phytoplankton Assemblages in Inshore–Offshore Gradients Using Flow Cytometry: A Case Study in the Eastern English Channel," *Journal of Marine Systems* 156 (2016): 76–85, https://doi.org/10.1016/j.jmarsys.2015.11.009.

58. M. Rijkeboer, "The Influence of (System) Temperature on Stability of Flow Cytometer Performance (RWS Information MEM2018-09; p. 13)," 2018.

59. S. Barrillon, R. Fuchs, A. A. Petrenko, et al., "Phytoplankton Reaction to an Intense Storm in the North-Western Mediterranean Sea," *Biogeosciences* 20, no. 1 (2023): 141–161, https://doi.org/10.5194/bg-20-141-2023.

60. M. Thyssen, S. Alvain, A. Lefèbvre, et al., "High-Resolution Analysis of a North Sea Phytoplankton Community Structure Based on in Situ Flow Cytometry Observations and Potential Implication for Remote Sensing," *Biogeosciences* 12, no. 13 (2015): 4051–4066, https://doi.org/10.5194/bg-12-4051-2015.

61. E. T. Buitenhuis, W. K. W. Li, D. Vaulot, et al., "Picophytoplankton Biomass Distribution in the Global Ocean," *Earth System Science Data* 4, no. 1 (2012): 37–46, https://doi.org/10.5194/essd-4-37-2012.

62. C. Gallot, "Best Practes for Automated Flow Cytometry: How to Optimize Cytograms. TT-CYTO Euromarine Workshop, LOG, Wimereux, France," (2024), https://doi.org/10.5281/zenodo.13827758.

63. L. Haraguchi, "Clustering of Different Areas. TT-CYTO Euromarine Workshop, LOG, Wimereux, France," (2024), https://doi.org/10.5281/zenodo.12819498.

64. L. Lanoy, "Automated Analytical Tools: API & Artificial Intelligence. TT-CYTO Euromarine Workshop, LOG, Wimereux, France," (2024), https://doi.org/10.5281/zenodo.13804988.

65. M. Libes, "Flow Cytometry Data Management Workflow at M.I.O. TT-CYTO Euromarine Workshop, LOG, Wimereux, France," (2024), https://doi.org/10.5281/zenodo.12547866.

66. M. Thyssen, "A FCM Dedicated Standard Vocabulary for Marine Microorganismes Naming. TT-CYTO Euromarine Workshop, LOG, Wimereux, France," (2024), https://doi.org/10.5281/zenodo.12571270.

Supporting Information

Additional supporting information can be found online in the Supporting Information section. **Data S1:** MIFlowCyt Item Checklist. **Figure S1:** Manually defined phytoplankton groups and "non-phytoplankton events" groups (larger or smaller than 1 μm beads, using 1 μm silica beads, not illustrated): (a) Total FLR versus Total FWS cytogram, (b) Total FLR versus Total FLO cytogram and (c) Max SWS versus Max FLR cytogram. Trigger level was set to FLR 6 mV. The sample was collected in the Bay of Marseille, at the SSL@MM station, and analyzed on instrument CS-2015-68. The separation of events larger and smaller than 1 μm silica beads is based on Total FWS (not shown), which explains the overlap in Max SWS between the two "non-phytoplankton events" groups. Groups are identified based on the recommended standard vocabulary and list of groups described in Section 2.2. Missing here are OraNano, HsNano, RedMicro, OraMicro, OraPico, RedRedPico, RedRedNano. These groups may be resolved analyzing larger volumes or in specific areas, or with an additional red laser. A detailed description of them can be found in [38]. **Figure S2:** Blank measurements correspond to acquisition files collected with the sample pump stopped, meaning the observed signal reflects a combination of the sheath fluid signature, electronic noise and some optical pollution. Two low trigger levels are illustrated to show the effects of lowering the trigger threshold on the increase of "non-phytoplankton events": (a) CS-2015-68 running sheath fluid only with a trigger threshold set to FLR 5 mV and PMT voltage to "Medium", generating an event rate of around 10,000 events s^{-1}; and (b) trigger threshold set to FLR 6 mV with similar PMT settings, generating an event rate below 50 events s^{-1}. The test was performed using salted sheath fluid with instrument CS-2015-68. **Figure S3:** Different trigger

thresholds on a natural sample from coastal waters off Boulogne-sur-Mer (Eastern English Channel) analyzed with instrument CS-2019-93. Trigger level (in mV) and event rate (event s^{-1}) are superimposed (average value during acquisition) (a) FLR 1 mV (b) FLR 1.25 mV (c) FLR 1.5 mV (d) FLR 2 mV. The separation of events larger and smaller than 1 μm silica beads is based on Total FWS (not shown), which explains the overlap in Max SWS between the two "non-phytoplankton events" groups. Measurement conditions (pump speed and measurement time) are identical between each tested trigger level. Groups are identified based on the recommended standard vocabulary and list of groups described in Section 2.2. **Figure S4:** Example of natural sea water acquisition using instrument CS-2015-68, changing PMT voltage and trigger thresholds. The three PMT presets ("Low", "Medium", "High") were combined with trigger thresholds on a natural sample collected at 50 m depth at the SOMLIT station in the Bay of Marseille, analyzed 1 h after collection at the SSL@MM. **Table S1:** Recommendations and best practices for CytoSense-type (CytoBuoy, NL) flow cytometers.